

# Radioiodine Therapy of Hepatoma Using Targeted Transfer of the Human Sodium/Iodide Symporter Gene

Libo Chen<sup>1,2</sup>, Annette Altmann<sup>2</sup>, Walter Mier<sup>3</sup>, Helmut Eskerski<sup>2</sup>, Karin Leotta<sup>2</sup>, Lihe Guo<sup>4</sup>, Ruisen Zhu<sup>1</sup>, and Uwe Haberkorn<sup>2,3</sup>

<sup>1</sup>Department of Nuclear Medicine, Shanghai Sixth People's Hospital, Shanghai Jiao Tong University, Shanghai, China; <sup>2</sup>Clinical Cooperation Unit Nuclear Medicine, German Cancer Research Center (DKFZ) and University of Heidelberg, Heidelberg, Germany; <sup>3</sup>Department of Nuclear Medicine, University of Heidelberg, Heidelberg, Germany; and <sup>4</sup>Division of Biochemistry and Cell Biology, Shanghai Institute for Biological Sciences, Chinese Academy of Sciences, Shanghai, China

We investigated the feasibility of radioiodine therapy targeting hepatoma cells (MH3924A) by tissue-specific expression of the human sodium/iodide symporter (hNIS) gene directed by the murine albumin enhancer and promoter (mAlb). **Methods:** The cell-specific transcriptional activity of mAlb was examined by a luciferase assay in several transiently transfected cell lines. MH3924A cells were stably transfected with the recombinant retroviral vector, in which hNIS complementary DNA expression was driven by mAlb and coupled to hygromycin resistance gene using an internal ribosomal entry site (IRES). Functional hNIS expression in hepatoma cells was confirmed by an iodide uptake assay. In imaging studies, the tumor-bearing ACI rats were intravenously injected with <sup>131</sup>I and imaged with a  $\gamma$ -camera. Biodistribution was studied at 30 min and at 1, 3, 6, and 25 h after injection of <sup>131</sup>I. Toxic effects of <sup>131</sup>I on hepatoma cells were studied in vitro and in vivo. **Results:** Stably transfected MH3924A cells concentrated <sup>125</sup>I up to 240-fold higher than the wild-type cells. The iodide uptake in stably transfected cells was inhibited by ouabain and sodium perchlorate but increased by 4,4'-diisothiocyanostilbene-2,2'-disulfonic acid. An in vitro clonogenic assay revealed an 86% decrease in colony number in stably transfected cells after exposure to 3.7 MBq/mL of <sup>131</sup>I and only about 8% in hNIS-negative control cells. Furthermore, the in vivo study showed intense tracer accumulation in hNIS-expressing tumors after administration of <sup>131</sup>I. At 3 h after intraperitoneal injection, the transfected tumors accumulated <sup>131</sup>I 19.2-fold higher than the parental tumors in a biodistribution study. Moreover, administration of a therapeutic dose of <sup>131</sup>I resulted in an inhibition of hNIS-expressing tumor growth, whereas control tumors continued to increase in size. **Conclusion:** A therapeutic effect of <sup>131</sup>I on hepatoma cells in vitro and in vivo has been demonstrated after tumor-specific iodide uptake induced by mAlb-directed hNIS gene expression. Because a stable transformed cell line has been used in these experiments, the clinical potential of this strategy must be evaluated after in vivo transfection of hepatoma cells.

**Key Words:** sodium/iodide symporter; radionuclide gene therapy; hepatoma; tissue-specific expression

**J Nucl Med 2006; 47:854–862**

**Y**ear 2000 estimates of the incidence of cancer indicate that primary liver cancer remains the fifth most common malignancy in men and the eighth in women. The incidence of hepatocellular carcinoma (HCC) is expected to continue to increase over the next 2 decades. The geographic areas at highest risk are located in Eastern Asia, Middle Africa, and some countries of Western Africa (1). Although surgery and percutaneous as well as transarterial interventions are effective in patients with limited disease (1–3 lesions, <5 cm in diameter), at the time of diagnosis >80% patients present with multicentric HCC and advanced liver disease or comorbidities that restrict the therapeutic measures to the best supportive care. Further, secondary HCC prevention after successful therapeutic interventions needs to be improved to make an impact on the survival of patients with HCC (2). Therefore, novel therapeutic strategies, including gene therapy, are urgently needed.

The sodium/iodide symporter (NIS), which is an intrinsic membrane glycoprotein with 13 putative transmembrane domains, plays an important role for the biosynthesis of thyroid hormones as it mediates the active transport of iodide into thyrocytes (3,4). NIS is critical for diagnosis and therapeutic management of thyroid diseases, including thyroid carcinoma. The cloning of the rat and human NIS genes in 1996 and extensive characterization of the NIS gene paved the way to novel radionuclide gene therapy strategies (5,6).

By targeted transfer and expression of the NIS gene, radioiodine treatment could be used to treat nonthyroid malignant disease as well as thyroid carcinoma. Radioiodine treatment exerts a bystander effect resulting from radiation crossfire, leading to the death of NIS-expressing cells as well as of the neighboring nontransfected cells (7).

Received Sep. 23, 2005; revision accepted Jan. 11, 2006.

For correspondence or reprints contact: Uwe Haberkorn, MD, Department of Nuclear Medicine, University of Heidelberg, Im Neuenheimer Feld 400, Germany 69120, Heidelberg.

E-mail: [uwe\\_haberkorn@med.uni-heidelberg.de](mailto:uwe_haberkorn@med.uni-heidelberg.de)

In addition, tumor-specific expression of the NIS gene has been performed with promising results in a variety of tumors, such as medullary thyroid carcinoma (8), prostate carcinoma (9,10), colon cancer (11), breast cancer (12), and neuroendocrine tumors (13). Transduction of NIS into hepatoma cell lines has also been reported after both stable plasmid transfection (14) and adenoviral infection using a nonspecific promoter (15).

Because systemic expression of NIS may cause severe adverse effects, it is important to manipulate gene expression such that it is expressed solely in cancer cells, thereby maximizing tumor-specific radioiodine accumulation and with minimal nonspecific uptake and radiation-induced toxic side effects in other organs. This may be done by specific transfection or by specific expression of the gene using tissue-specific regulatory elements. Transcriptional targeting of therapeutic genes reduces extratumoral toxicity and results in selective, tissue-specific expression of the therapeutic gene (16).

In the adult, albumin is expressed uniquely in the liver and in HCC mediated by transcriptional regulation. The albumin enhancer and promoter have been successfully used in the past to target expression of therapeutic genes to tumor tissues that express the protein (17–19).

In this study, we developed a human NIS (hNIS) gene expression system, based on liver-specific regulatory elements on a self-inactivating retroviral vector. After transfer of the hNIS gene into a rat Morris hepatoma cell line (MH3924A), iodide uptake and efflux were determined under various conditions, and the therapeutic effect was evaluated both in vitro and in vivo. The results reported here demonstrate the potential efficacy of radioiodine therapy of hepatoma after retrovirus-mediated transfer of hNIS gene under the control of the albumin gene enhancer and promoter.

## MATERIALS AND METHODS

### Plasmid Constructs

Recombinant retroviral plasmid pSIRmAlb<sup>h</sup>NISIVSIREShyg was constructed by standard plasmid subcloning techniques. In brief, murine albumin enhancer and promoter (mAlb) was removed from the bluescript vector, which was kindly provided by Dr. Richard D. Palmiter (20), by restriction digestion using *Not* I and *Bam*HI, agarose-gel purified, and ligated into the vector pSKhNISIVSIREShyg. After restriction digestion with *Xba* I and *Xho* I, a fragment containing mAlb, hNIS, intervening sequence ([IVS] a synthetic intron), internal ribosomal entry site (IRES), and hygromycin resistance gene was ligated into a bicistronic retroviral vector based on the pSIR self-inactivating retroviral vector (Clontech). The self-inactivating vector contains a 176-base pair deletion in the 3' long terminal repeat (LTR) that removes retroviral enhancer sequences (21). After reverse transcription, the 3' LTR is copied and replaces the 5' LTR, thereby inactivating the 5' LTR promoter and leaving mAlb as the only promoter and enhancer that drive the expression of downstream-located genes.

To assess the function and cell specificity of mAlb, the AP1 enhancer and the TATA-like promoter (P<sub>TAL</sub>) region of pAPI-Luc

(Clontech) were replaced by mAlb with molecular clonal techniques, and pmAlb-Luc containing the luciferase gene under the control of mAlb was constructed. The plasmid pAPI-Luc was used as a control vector to monitor transfection and expression efficiency and to normalize the levels of luciferase expression in different cell lines.

The resulting recombinant plasmids were purified and their sequences were confirmed by restriction digestion and DNA sequencing. The plasmid concentration was determined by spectrophotometry.

### Cell Culture

The rat Morris hepatoma cell line MH3924A was cultured in RPMI 1640 medium with glutamax-I supplemented with 20% fetal calf serum (FCS); the cell line SW1736 (human anaplastic thyroid carcinoma) was grown in RPMI 1640 medium with glutamax-I supplemented with 10% FCS. The cell lines MCF-7 (human mammary adenocarcinoma), LCLC-103H (human large cell lung carcinoma), and the transient packaging cell line EcoPake293, used for the production of ecotropic retroviral particles, were cultured in Dulbecco's modified Eagle medium (DMEM) with 10% FCS. All cells were maintained at 37°C, in an atmosphere of 95% air and 5% CO<sub>2</sub>.

### Transient and Stable Transfection

Before transient transfections, MH3924A, SW1736, MCF-7, and LCLC-103H cells were grown to 50%–70% confluency and transfected with purified recombinant plasmid pmAlb-Luc or pAPI-Luc using lipofectamine plus reagent (Invitrogen) according to the manufacturer's instructions. After transfections, cells were incubated for 24 h in growth medium followed by measurement of luciferase activity and the protein content.

To establish hepatoma cell lines stably expressing hNIS gene, transient packaging of the recombinant retroviral vector was performed using EcoPack293 cells. After 2 d, the medium containing the retroviral particles was centrifuged and filtered to remove detached packaging cells and used for the infection of the MH3924A cells in the presence of 8 µg/mL Polybrene (Sigma-Aldrich) overnight. To select for the cells infected with retroviral particles containing the hNIS gene and hygromycin resistance gene, the cells were treated with 425 µg/mL hygromycin for 3 wk until resistant cell lines were established.

### Luciferase Assay

Twenty-four hours after transfection with luciferase reporter plasmid pmAlb-Luc or control plasmid pAPI-Luc, the transiently transfected MH3924A and control cell lines were washed twice with phosphate-buffered saline (PBS) and lysed with passive lysis buffer (Promega). The luciferase activities were measured using the Dual-Luciferase Reporter Assay System (Promega) according to the manufacturer's recommendations. A luminescence reader Luminoskan Ascent was programmed to perform a 2-s premeasurement delay, followed by a 10-s measurement period for each reporter assay. Firefly luciferase activity was assayed by injecting 100 µL Luciferase Assay Reagent II (Promega) into 20 µL passive lysis buffer lysate. Relative luciferase activity was expressed as the percentage of pmAlb-Luc value compared with pAPI-Luc value, normalized to the protein content.

### Iodide Uptake and Efflux Studies

The iodide uptake was performed as described previously (22–24). All experiments were done in triplicate and repeated at least

twice. A total number of  $4\text{--}5 \times 10^5$  wild-type MH3924A tumor cells or recombinant cells were incubated in 1 mL culture medium containing 74 kBq  $\text{Na}^{125}\text{I}$  (Amersham; specific activity, 625 MBq/ $\mu\text{g}$ ) for 1 h. The cells were then washed twice with ice-cold PBS and lysed with 0.3 mol/L sodium hydroxide on ice. The radioactivity in cell lysates was measured using an automated NaI(Tl) well counter (Cobra II; Canberra Packard). The recombinant cell line named MHmAlbhNIS, which showed the highest iodide uptake, was used in the following experiments. The cell counts were determined in a Coulter Counter (Beckman Coulter). The cell viability was assessed by trypan blue staining.

To determine the iodide uptake in relationship to the incubation time, the recombinant cell line MHmAlbhNIS and wild-type MH3924A cells were cultured with 74 kBq  $\text{Na}^{125}\text{I}$  for 2, 5, 10, 20, or 30 min or 1, 2, or 4 h. Washing and counting were performed as described.

For modulation of the iodide uptake, hNIS-expressing and wild-type cells were incubated for 1 h in medium containing  $\text{Na}^{125}\text{I}$  (74 kBq) or  $\text{Na}^{125}\text{I}$  medium supplemented with 50  $\mu\text{mol/L}$  sodium perchlorate (Sigma), 100  $\mu\text{mol/L}$  of the anion channel blocker 4,4'-diisothiocyano-2,2'-disulfonic acid (DIDS; Sigma), or 500  $\mu\text{mol/L}$  ouabain (Sigma), an inhibitor of the  $\text{Na}^+/\text{K}^+$ -adenosine triphosphatase ( $\text{Na}^+/\text{K}^+$ -ATPase). Thereafter, the cells were washed, lysed, and counted as described.

To determine the  $^{125}\text{I}^-$  efflux, recombinant cells were incubated for 1 h with medium containing 74 kBq  $\text{Na}^{125}\text{I}$ . After the cells had been washed twice, 3 wells were lysed immediately. Fresh non-radioactive medium was added to the remaining wells. The cells were again incubated for 10, 20, or 30 min and lysed as described.

To investigate the effect of lithium and DIDS on the  $^{125}\text{I}^-$  efflux, cells were incubated for 24 h with 10 mmol/L lithium chloride (Merck) or supplemented with 300  $\mu\text{mol/L}$  DIDS just before adding the  $^{125}\text{I}^-$ . Thereafter, an efflux experiment was performed as described above. After incubation for 1 h in the presence of 74 kBq  $\text{Na}^{125}\text{I}$ , the radioactive medium was removed, and the cells were washed twice and incubated in nonradioactive lithium- or DIDS-containing medium for 10, 20, or 30 min and lysed.

### In Vitro Clonogenic Assay

The procedure was performed as described by Mandell et al. (25) with minor modifications. In brief, cells were grown in a 6-well plate and incubated for 7 h at  $37^\circ\text{C}$  with 1 mL culture medium containing 0.925, 1.85, or 3.7 MBq/mL of  $\text{Na}^{131}\text{I}$ . The uptake was terminated by removing the radioisotope-containing medium and washing the cells twice with culture medium. The cells were then trypsinized, counted, and plated at densities of 250 or 1,000 cells per well with culture medium in 6-well plates. The cells were grown for 8 d, fixed with 3:1 methanol/acetic acid, and stained with crystal violet solution (Sigma), and the number of macroscopic colonies was counted. Parallel experiments were performed for each cell line using medium without  $^{131}\text{I}^-$ , and all values were adjusted for plating efficiency. Survival rate was calculated as the percentage of colony number in a plate treated with  $\text{Na}^{131}\text{I}$  compared with the number in a plate with mock treatment.

### Animal Model

The experiments involving animals were performed in compliance with the current version of the national law on the Protection of Animals. Biodistribution and imaging studies were performed under general gaseous anesthesia (40%  $\text{O}_2$ /60%  $\text{N}_2\text{O}$ /1% halothane). The generation of subcutaneous tumors was performed as

follows:  $5 \times 10^6$  MHmAlbhNIS tumor cells suspended in 0.1 mL OptiMEM medium (Invitrogen) were transplanted subcutaneously into the right thigh and  $4 \times 10^6$  wild-type MH3924A cells were inoculated subcutaneously into the left thigh of 6-wk-old male ACI rats weighing 200–250 g. For therapy experiments, 1 group of 15 rats was inoculated subcutaneously with  $5 \times 10^6$  MHmAlbhNIS tumor cells, and a second group of 15 rats was implanted subcutaneously with  $4 \times 10^6$  wild-type MH3924A cells. Each group was then divided into 3 subgroups in terms of  $^{131}\text{I}$  administration—namely, 5 rats for negative control, 5 rats for intraperitoneal injection of  $^{131}\text{I}$ , and 5 rats for intravenous injection of  $^{131}\text{I}$ . Rats with tumor reaching a volume  $>8,000 \text{ mm}^3$  were euthanized.

### Biodistribution of $\text{Na}^{131}\text{I}$ in Tumor-Bearing Rats

At 30 min and at 1, 3, 6, and 25 h after intraperitoneal administration of  $\text{Na}^{131}\text{I}$  (7.4 MBq/rat), the animals were sacrificed. Tumor, blood, and selected tissues (heart, lung, spleen, liver, kidney, muscle, brain, bone, skin, stomach, intestine, thyroid gland) were dissected, blotted dry, weighted, and measured. For radioactivity measurement, an automated NaI(Tl) well counter (Cobra II; Canberra Packard) was used. Results are expressed as the percentage of injected dose per gram (%ID/g) of tissue.

### Tumor Imaging

For imaging studies, only animals bearing tumors with a minimum size of 10 mm in diameter were accepted. After injection of  $\text{Na}^{131}\text{I}$  (7.4 MBq/rat) in 200  $\mu\text{L}$  of 0.9% NaCl into the lateral tail vein, scintigraphic images were taken using a 15-in scintillation camera (Searle-Siemens). The time-dependent relative accumulation of radioactivity in different regions of interest was monitored dynamically within 30 min after tracer administration and static images at 30 min and at 1, 2, 4, and 24 h after injection were acquired in 5 animals.

### $^{131}\text{I}$ Therapy In Vivo

A single administration of  $\text{Na}^{131}\text{I}$  (148 MBq/rat) in 200  $\mu\text{L}$  of 0.9% NaCl was injected intraperitoneally or intravenously when the tumors grew to 0.6–1.0 cm in diameter. The tumor size was monitored before administration of radioiodine and every 3 d thereafter by measuring 2 diameters with a caliper and then converted to volume by the formula  $4/3 \times \pi r^3$  ( $r$  = sum of the 2 diameters divided by 4) (26). All rats were followed for a total of 3 wk and then euthanized.

### Statistical Analysis

All experiments were performed in triplicates unless otherwise indicated. The results are presented as mean  $\pm$  SD. Statistical significance was tested using the Student *t* test procedure, which was realized using SigmaPlot version 9.0 (Jandel Scientific). *P* values  $< 0.05$  were considered as statistically significant.

## RESULTS

### Luciferase Assay

To assess the cell-specific transcriptional activity of the albumin enhancer/promoter a reporter gene assay using luciferase was performed in several transiently transfected cells. The transient transfection showed that the mAlb resulted in preferential expression of luciferase gene in hepatoma cells, with negligible expression in albumin-negative cell lines, such as SW1736, MCF-7, and LCLC-103H (Fig. 1).

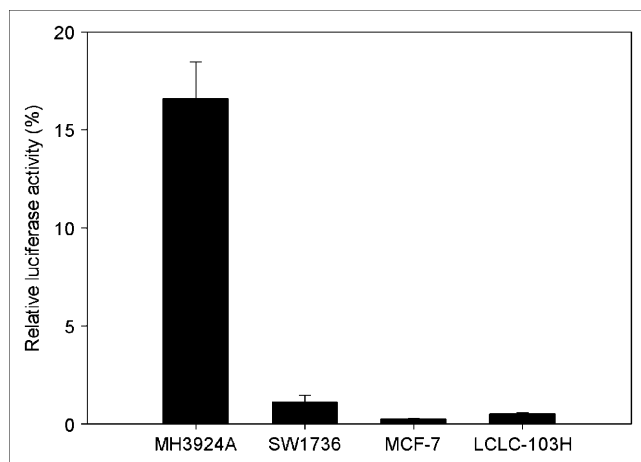


**FIGURE 1.** Expression of reporter gene (luciferase) driven by albumin enhancer/promoter in different cell lines. Data are expressed as mean  $\pm$  SD ( $n = 3$ ).

### Iodide Uptake Studies

After infection of MH3924A cells with the recombinant retroviruses and selection with hygromycin, 9 stable cell lines were established. The range of relative iodide uptakes among these cell lines was 93- to 240-fold higher than that of the parental cells. The iodide uptake by MHmAlbhNIS cells was rapid, reaching a half-maximal level within 5 min and a plateau at 20–30 min, as shown in Figure 2A. After incubation for 1 h, up to 240-fold more  $^{125}\text{I}^-$  was transported into the hNIS-expressing hepatoma cells compared with that of the parental cells.

Figure 2B presents the effect of DIDS, ouabain, and sodium perchlorate on iodide uptake in MHmAlbhNIS cells. The specific NIS inhibitor, sodium perchlorate, showed an inhibitory effect on the iodide accumulation in the MHmAlbhNIS cells by 93.65% ( $P < 0.01$ ). Ouabain, an inhibitor of  $\text{Na}^+/\text{K}^+$ -ATPase, led to a loss of 89.14% of the iodide uptake ( $P < 0.01$ ). However, in the presence of 100  $\mu\text{mol/L}$  DIDS, an anion channel blocker, we observed an opposite effect, as it increased the iodide accumulation in the genetically modified cells by 16.15% ( $P < 0.01$ ).

### Iodide Efflux Studies

To determine the iodide efflux, the iodide uptake was permitted to proceed for 1 h, when a steady-state level of accumulation was achieved, as is demonstrated by Figure 1A. As shown in Figure 3, the amount of remaining  $^{125}\text{I}^-$  in the MHmAlbhNIS cell lysates was determined as a function of time after replacement of the uptake medium by nonradioactive medium. The cellular radioactivity was continuously released to the medium, resulting in an effective half-life of approximately 15 min and 80% efflux after 30 min. In the presence of  $\text{Li}^+$  ion or DIDS, the rapid iodide efflux was not postponed. However, the addition of 10 mmol/L lithium led to an inhibition of 50% in the iodide uptake as compared with cells without lithium.

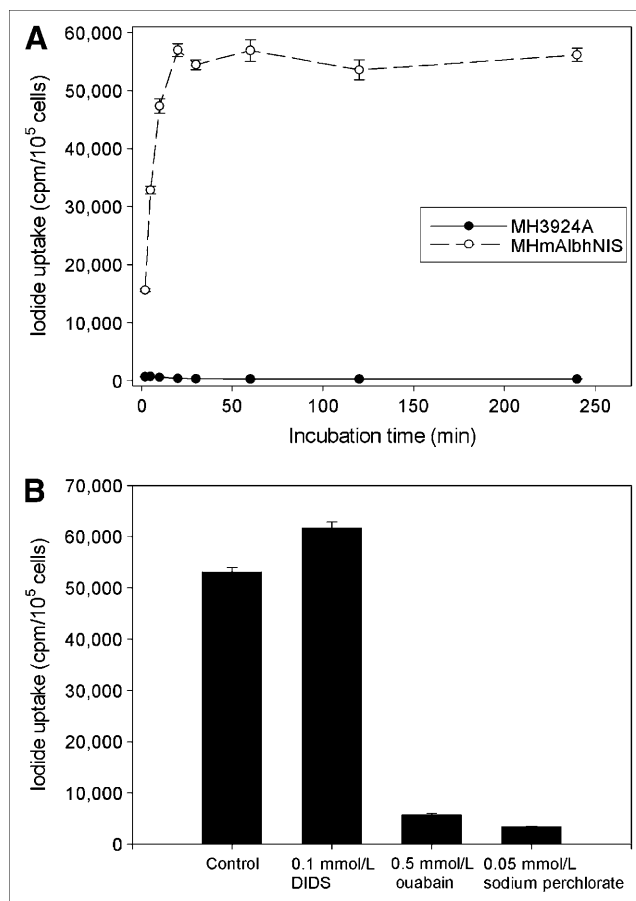


**FIGURE 2.** Time course of iodide uptake by MH3924A and MHmAlbhNIS cells (A) and modulation of iodide uptake by DIDS, ouabain, and sodium perchlorate (B). Data are expressed as mean  $\pm$  SD ( $n = 3$ ).

### In Vitro Clonogenic Assay

Using an in vitro clonogenic assay, we investigated whether  $^{131}\text{I}^-$  showed selective cytotoxic activity in NIS-expressing cells and wild-type cells. As shown in Figure 4, after treating with 0.925, 1.85, or 3.7 MBq/mL of  $\text{Na}^{131}\text{I}$

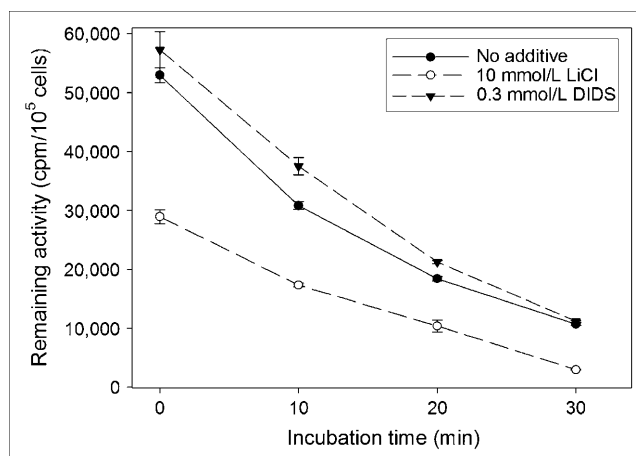


**FIGURE 3.** Iodide efflux from MHmAlbhNIS cells after 1-h incubation with  $\text{Na}^{125}\text{I}$ . Data are expressed as mean  $\pm$  SD ( $n = 3$ ).

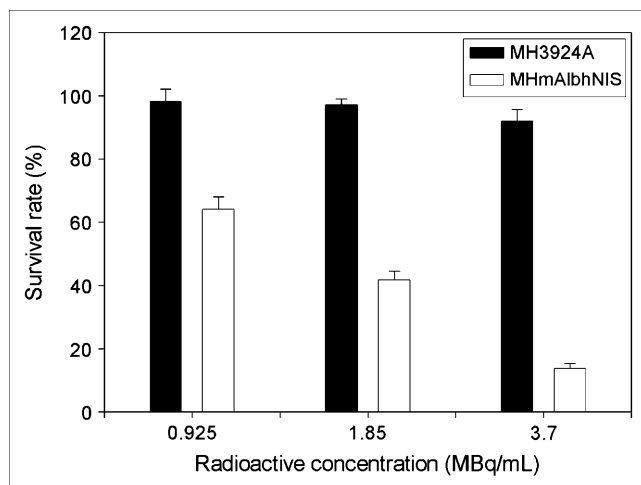


**FIGURE 4.** Survival rates (%) of MH3924A and MHmAlbhNIS cells treated with  $\text{Na}^{131}\text{I}$ . Data are expressed as mean  $\pm$  SD ( $n = 3$ ).

for 7 h, the clonogenic survival rates of MHmAlbhNIS cells were markedly reduced in a dose-dependent manner to  $64.03\% \pm 3.98\%$ ,  $41.81\% \pm 2.75\%$ , and  $13.74\% \pm 1.57\%$ , respectively. The survival rates of wild-type MH3924A cells were  $98.18\% \pm 3.91\%$ ,  $97.18\% \pm 1.82\%$ , and  $91.98\% \pm 3.71\%$ , respectively. These data indicate that a sufficiently high dose of radiation was achieved in NIS-transfected hepatoma cells to result in cell killing at a dose that spared parental cells, which are unable to trap  $^{131}\text{I}^-$ . The enhanced cell killing of the transfected versus the wild-type cells maybe due to a steady state of relatively high radioiodide accumulation resulting from 7 h of continuous exposure.

### Tumor Imaging

Consistent with the data obtained from the in vitro studies, the hNIS-expressing tumor tissue accumulated  $^{131}\text{I}^-$  rapidly and significantly, leading to scintigraphic visualization, whereas the control tumor was not visualized (Fig. 5). Normal NIS-expressing tissues, including those of salivary gland, thyroid gland, and stomach, were also clearly visible.

### Biodistribution of $\text{Na}^{131}\text{I}$ in Tumor-Bearing Rats

The biodistribution data for  $^{131}\text{I}^-$  administered intraperitoneally in MHmAlbhNIS- and MH3924A-bearing ACI rats are summarized in Figure 6. The NIS-expressing tumors exhibited an increased uptake of  $^{131}\text{I}^-$  versus the parental MH3924A tumors. The quantitation of the  $^{131}\text{I}^-$  uptake (%ID/g) in the tumors and various organs was evaluated at 30 min and at 1, 3, 6, and 25 h after tracer administration. In the hNIS-expressing tumors, up to 19.2-fold higher iodide accumulation was detected at 3 h after administration when compared with the wild-type tumors, corresponding to  $4.63 \pm 1.63$  %ID/g. The  $^{131}\text{I}^-$  uptake in the wild-type tumors at 3 h after intraperitoneal injection was  $0.24 \pm 0.02$  %ID/g. As a positive control,  $42.19 \pm 8.08$  %ID/g could be achieved in the thyroid gland at 3 h

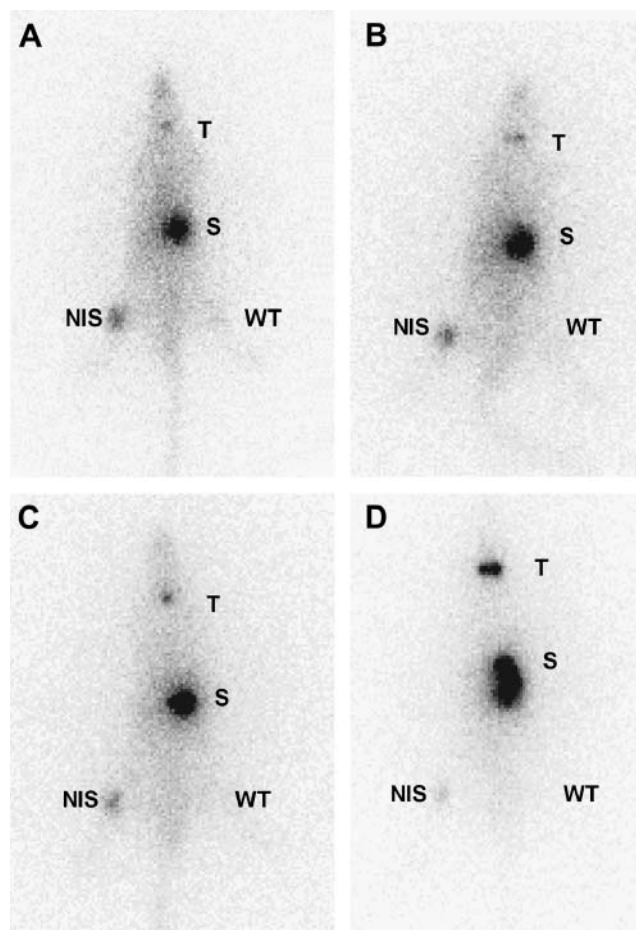


**FIGURE 5.** Whole-body scintigraphic images (anterior view) of ACI rats subcutaneously transplanted with hNIS-expressing (right thigh) or wild-type Morris hepatoma cells (left thigh) at 30 min (A), 2 h (B), 4 h (C), and 24 h (D) after intravenous injection of  $^{131}\text{I}^-$ . T = thyroid; S = stomach; NIS = NIS-expressing tumor; WT = wild-type tumor.

after tracer administration (data not shown). The radioactivity remained quite stable in the NIS-expressing tumors for 6 h, followed by a decline during the period until 25 h after tracer administration. We also obtained biodistribution data after intravenous administration of  $\text{Na}^{131}\text{I}$ . There was no significant difference in the biodistribution between the 2 routes of administration at the selected time points (data not shown).

### Radioiodine Therapy Study In Vivo

Although the subcutaneous tumors generated in ACI rats by implanting hepatoma cells infected with the recombinant retrovirus showed no significant shrinkage, the tumor growth was retarded significantly after treatment with  $\text{Na}^{131}\text{I}$ , whereas the wild-type tumor rapidly increased in size (Fig. 7). On the 21st day, the difference in tumor volume between the 2 treatment subgroups inoculated with parental and genetically modified cells was statistically significant. In contrast, the difference of tumor volume

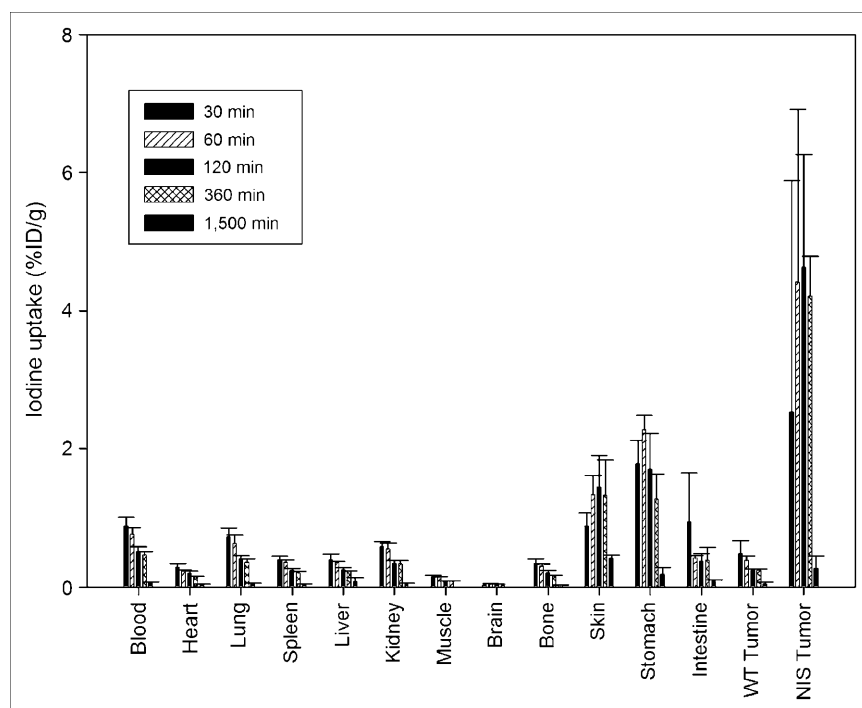


**FIGURE 6.** Biodistribution of radio-tracer at different times after intraperitoneal administration of  $\text{Na}^{131}\text{I}$  in ACI rats bearing MH3924A and MHmAlbNIS tumor cells. Data are expressed as mean %ID/g  $\pm$  SD ( $n = 3$ ). WT = wild-type tumor (MH3924A).

between the 2 treatment subgroups administrated intraperitoneally and intravenously bearing the same tumor cell line (MH3924A or MHmAlbNIS) showed no statistical significance, indicating no dependence of treatment effects on the administration route.

## DISCUSSION

Benign thyroid diseases and thyroid cancer can be effectively diagnosed and treated by radioiodine, which is due to the expression of thyroid-specific genes such as NIS, thyroid peroxidase (TPO), and thyroglobulin (Tg). These proteins lead to trapping and organification of radioactive iodine in the target tissues. After the cloning of the NIS gene, several investigators explored the capacity of NIS gene transfer to induce radioiodine accumulation in non-thyroidal tumor cells, including hepatoma (14,22,27).

In recent years, a variety of gene therapy approaches have been examined in hepatoma, such as corrective gene therapy for the induction of apoptosis, cytoreductive gene therapy including the herpes simplex virus thymidine kinase/ganciclovir system, and immunomodulatory gene therapy using numerous cytokine genes. More recently, the cloning and characterization of NIS gene provided a possibility of radionuclide gene therapy for nonthyroid cancers using NIS gene transfer combined with the application of radioactive isotopes, such as  $^{131}\text{I}$ ,  $^{188}\text{Re}$ , and  $^{211}\text{At}$  (14).

On the other hand, tissue-specific expression of therapeutic genes of interest has been proven to be an extremely attractive strategy in gene therapy. One effective way to direct transgene expression to specific tissues or tumors is

the use of tissue-specific promoters, thereby maximizing tissue-specific cytotoxicity and reducing extratumoral side effects. As far as NIS gene is concerned, Kakinuma et al. (9) and Spitzweg et al. (10) reported radioiodine accumulation and therapeutic effectiveness of  $^{131}\text{I}$  in prostate cancer cells (LNCaP) after induction of tissue-specific iodide uptake activity by prostate-specific antigen promoter-directed NIS expression in vitro and in vivo. Thereafter, Scholz et al. (11) investigated the feasibility of using radioiodine therapy in colon carcinoma cells (HCT 116) after tumor-specific expression of the hNIS using the carcinoembryonic antigen promoter, and an in vitro therapeutic effect of  $^{131}\text{I}^-$  has been demonstrated. Herein, tissue-specific activity of mAlb was demonstrated by transient expression of a luciferase reporter gene in several cell lines.

In the current study we chose hepatoma as a tumor model unresponsive to  $^{131}\text{I}^-$  therapy due to the lack of iodide uptake to investigate the potential of NIS gene transfer as a therapeutic strategy. To target NIS gene expression to hepatoma cells, the mAlb were applied to direct the hNIS gene expression. Because the albumin gene is regulated in a tissue-specific manner, the albumin promoter together with its enhancer represents an ideal means for hepatoma cell-specific gene expression and, therefore, has been used in a variety of studies to target therapeutic gene to hepatoma (16–19). The combination of the albumin promoter/enhancer with a retroviral vector system, which infects only dividing cells, ensures that normal liver cells are not affected.

The results presented here show that the albumin enhancer and promoter are capable of driving functional NIS

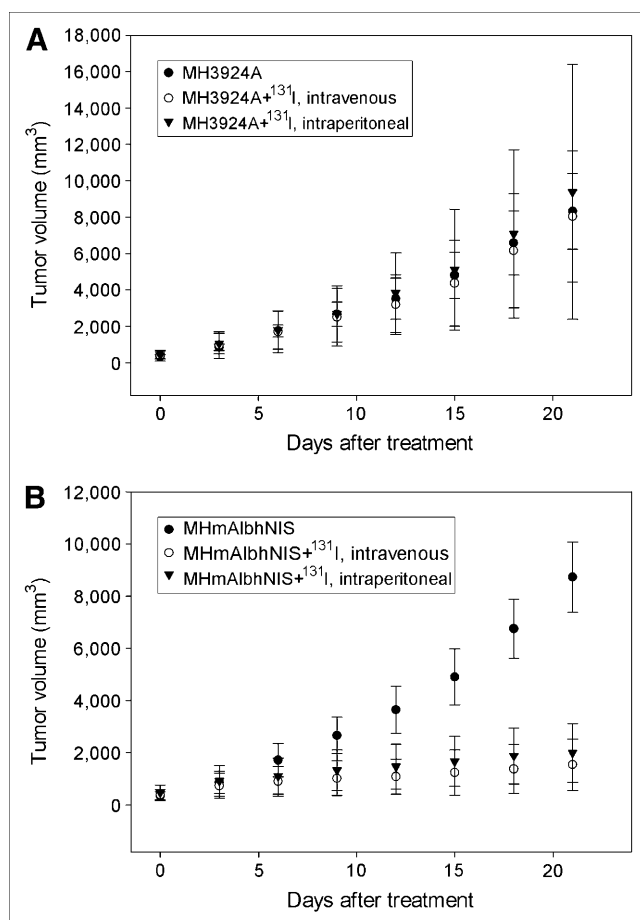


**FIGURE 7.** Antitumor effect of hNIS expression combined with radioiodide administration in ACI rats injected subcutaneously with wild-type MH3924A cells (A) or MHmAlbhNIS tumor cells (B). Data are expressed as mean  $\pm$  SD ( $n = 5$ ).

expression. We observed perchlorate- and ouabain-inhibitable iodide uptake up to 240-fold over that of the wild-type cells. Although, as mentioned previously, there have been other studies using the albumin gene enhancer and promoter to target therapeutic genes to a variety of tumor types, NIS provides a significant advantage, as it allows for noninvasive  $^{123}\text{I}$ ,  $^{124}\text{I}$ ,  $^{131}\text{I}$ , or  $^{99\text{m}}\text{Tc}$  imaging to confirm correct targeting of the gene before proceeding to radionuclide therapy. In vivo investigations confirmed the potential of this construct for the imaging of NIS expression in hepatoma.

Finally, the amount of accumulated  $^{131}\text{I}^-$  was shown to be sufficiently high to elicit a significant dose-dependent therapeutic effect in an in vitro clonogenic assay with a selective killing effect of approximately 86% of NIS-expressing hepatoma cells as compared with only 8% of parental cells at the radioactive concentration of 3.7 MBq/mL. Our data on  $^{131}\text{I}^-$  therapy in vivo demonstrated inhibition of tumor growth after hNIS gene transfer combined with intraperitoneal or intravenous administration of a single therapeutic dose of  $^{131}\text{I}^-$ . These data suggest that the intratumoral radioiodine concentration compensated the low biologic

half-life to a certain degree, thereby achieving a therapeutically effective radiation dose in the NIS-expressing tumors. In addition, the energy emitted by  $^{131}\text{I}^-$  accumulated in NIS-expressing cells through  $\beta$ -particles may result in a substantial crossfire effect. Further, we found no difference in therapy effects between the intravenous and the intraperitoneal application, indicating no dependence of treatment effects on the administration route.

However, as shown in the iodide efflux experiments,  $^{125}\text{I}^-$  in the genetically modified cells is continuously released into the medium, resulting in an effective half-life of 15 min, which could not be postponed by the presence of  $\text{Li}^+$  ion or DIDS. The short retention time of radioiodide observed in cells in culture and xenografts, combined with the relatively long physical half-life of  $^{131}\text{I}$ , probably results in an insufficient absorbed dose for successful tumor eradication.

Fortunately, in addition to iodide, several anions, such as  $\text{ClO}_4^-$ ,  $\text{ReO}_4^-$ ,  $\text{SCN}^-$ ,  $\text{ClO}_3^-$ , and  $\text{Br}^-$ , are transported by NIS (28). It has been reported that NIS-expressing tissues and cells could concentrate pertechnetate ( $\text{TcO}_4^-$ ), perrhenate ( $\text{ReO}_4^-$ ), or astatide ( $\text{At}^-$ ). Some research groups have proposed to use  $^{188}\text{Re}$ -perrhenate in the treatment of NIS-expressing tumors as an alternative to  $^{131}\text{I}$  (29), because  $^{188}\text{Re}$ -perrhenate is a powerful  $\beta$ -emitting radiometal and is conveniently obtained from an  $^{188}\text{W}/^{188}\text{Re}$  generator. Moreover,  $^{188}\text{Re}$ -perrhenate has excellent physical properties and emission characteristics.

Furthermore, astatine, the heaviest of the halogens, exhibits a pronounced accumulation in the thyroid gland in halide form and in the stomach (30). The use of radionuclides with similar chemical properties and more favorable physical properties, such as a higher linear energy transfer and shorter physical half-life, should result in an increased radiation dose and, thus, enhanced efficacy. Another advantage of  $\alpha$ -particle therapy is that cell survival is independent of the dose rate, which is of particular significance in relation to the rapid uptake and efflux kinetics of radiohalides in NIS-expressing cells lacking an organification mechanism. Because we observed a stable accumulation of iodine during the first 6 h after tracer administration,  $^{211}\text{At}$  may be a promising treatment strategy for the therapy of NIS-expressing tumors as suggested by others (31,32). However, the short tissue range of the  $\alpha$ -particles represents a disadvantage in larger tumors, where heterogeneity in hemodynamics as well as heterogeneity of the transgene expression levels is found. This problem is even more pronounced in face of the low, and possibly varying, transfection efficiency of viral vectors in vivo. Therefore,  $^{211}\text{At}$  is suggested for minimal disease situations where tumor burden is lowest, such as micrometastasis or residual tumor margins after surgical debulking. Carlin et al. (32) observed a higher nonspecific uptake of  $^{211}\text{At}$  than  $^{131}\text{I}$  in cells lacking NIS expression, which contributed to a lower absorbed dose ratio between NIS-transfected and nontransfected cells. This may result in a higher dose in

nontarget tissues. Furthermore, biodistribution studies with  $^{211}\text{At}$  showed a significantly higher uptake in lung and spleen with concerns over radiotoxicity in these tissues.

The use of other radionuclides such as  $^{188}\text{RO}_4$  or  $^{125}\text{I}$  has been studied by Shen et al. (33). The authors found a prolonged survival of glioma-bearing rats when using  $^{188}\text{RO}_4$ , which was explained by the greater energy release in a short time interval. A combination of Auger and  $\beta$ -emission may profit from multiple emission ranges that span variations in tumor size and circumvent a nonuniform absorbed-dose distribution. A cocktail approach using 296 MBq (8 mCi) of each  $^{125}\text{I}$  and  $^{131}\text{I}$  was found to be as effective as 592 MBq (16 mCi)  $^{131}\text{I}$ .

Alternative methods of targeted delivery of radioactivity to cancer cells involve conjugation of radionuclides to agents that have specific affinity for tumor markers. Gene transfer has been used to induce tumor cells to express elevated levels of surface antigens, receptors, or transporters to enhance targeting by radiolabeled antibodies, peptides, or metaiodobenzylguanidine, respectively (34–36). Unlike these schemes for radionuclide targeting,  $\text{Na}^{131}\text{I}$  therapy requires no radiochemical synthetic procedure. In contrast to antibodies, radioiodine is nonimmunogenic and has ideal diffusion properties. Whereas tumor targeting using radiolabeled antibodies and peptides has just recently reached the clinical application, the administration of  $\text{Na}^{131}\text{I}$  has for a long time been proven to be effective in the eradication or control of thyroid carcinoma. Therefore, NIS gene transfer, followed by radioiodine administration, allows the possibility of treatment of hepatoma in a manner analogous to the highly efficacious treatment of differentiated thyroid carcinoma with radioiodide. Because intense accumulation of the tracer is expected to occur in the thyroid, clearly an ablation of the thyroid has to precede a radioiodine treatment for hepatoma.

It is very unlikely that gene therapy technology will achieve 100% transfection of cells in a tumor in situ. Therefore, 2 types of effects are important with respect to enhancement of therapeutic efficacy (37): the cross-fire effect on cells that are not accumulating the tracer and the radiation-induced bystander effect (RIBE). RIBE describes a situation in which cells that have not been directly exposed to ionizing radiation behave as though they have been exposed: they die or show chromosomal instabilities or other abnormalities. Although the exact mechanism of RIBE is unclear, there is evidence that chemical signaling processes transmit information from irradiated cells to neighboring cells. Therefore, these effects are an important requirement for effective gene therapy, particularly when transfection efficiencies are low. Because the radiologic bystander effect resulting from radiation crossfire provides exciting possibilities (7,38), an in vivo transduction using this recombinant retrovirus or other viral vectors to test the feasibility of this radionuclide gene therapy strategy toward clinical application must be performed in further studies. However, these will rely on the improvement of currently available vector systems.

## CONCLUSION

Tumor-specific radioiodine accumulation and therapeutic effectiveness of  $^{131}\text{I}$  on hepatoma cells have been observed in vitro and in vivo after mAlb-directed hNIS transfer and expression via a recombinant self-inactivating retroviral vector. This study demonstrates the potential of hNIS as a therapeutic gene allowing radioiodine therapy for hepatoma after tissue-specific gene transfer. Because a 100% transfection rate in vivo is very unlikely, further efforts must concentrate on the improvement of the gene delivery systems. Future studies will focus on enhancing the therapeutic effects via combination treatment using antiangiogenesis agents or chemotherapy.

## ACKNOWLEDGMENTS

The authors are grateful to Dr. Richard D. Palmiter (Howard Hughes Medical Institute and Department of Biochemistry, University of Washington, Seattle, WA) for supplying the plasmid containing mAlb. We thank Iris Morr, Miriam Mahmut, Uschi Schierbaum, Gabriela Glensch, Ulrike Hebling, and Sigrid Peschke for their technical help and also thank Dr. Johannes Hoffend and Tianjin Liu for their helpful discussions.

## REFERENCES

1. Bosch FX, Ribes J, Cleries R, Diaz M. Epidemiology of hepatocellular carcinoma. *Clin Liver Dis*. 2005;9:191–211.
2. Blum HE. Treatment of hepatocellular carcinoma. *Best Pract Res Clin Gastroenterol*. 2005;19:129–145.
3. De La Vieja A, Dohan O, Levy O, Carrasco N. Molecular analysis of the sodium/iodide symporter: impact on thyroid and extrathyroid pathophysiology. *Physiol Rev*. 2000;80:1083–1105.
4. Spitzweg C, Heufelder AE, Morris JC. Thyroid iodine transport. *Thyroid*. 2000;10:321–330.
5. Dai G, Levy O, Carrasco N. Cloning and characterization of the thyroid iodide transporter. *Nature*. 1996;379:458–460.
6. Smanik PA, Liu Q, Furminger TL, et al. Cloning of the human sodium iodide symporter. *Biochem Biophys Res Commun*. 1996;226:339–345.
7. Carlin S, Cunningham SH, Boyd M, McCluskey AG, Mairs RJ. Experimental targeted radioiodide therapy following transfection of the sodium iodide symporter gene: effect on clonogenicity in both two- and three-dimensional models. *Cancer Gene Ther*. 2000;7:1529–1536.
8. Cengic N, Baker CH, Schutz M, Goke B, Morris JC, Spitzweg C. A novel therapeutic strategy for medullary thyroid cancer based on radioiodine therapy following tissue-specific sodium iodide symporter gene expression. *J Clin Endocrinol Metab*. 2005;90:4457–4464.
9. Kakinuma H, Bergert ER, Spitzweg C, Cheville JC, Lieber MM, Morris JC. Probasin promoter (ARR<sub>2</sub>PB)-driven, prostate-specific expression of the human sodium iodide symporter (h-NIS) for targeted radioiodine therapy of prostate cancer. *Cancer Res*. 2003;63:7840–7844.
10. Spitzweg C, O'Connor MK, Bergert ER, Tindall DJ, Young CY, Morris JC. Treatment of prostate cancer by radioiodine therapy after tissue-specific expression of the sodium iodide symporter. *Cancer Res*. 2000;60:6526–6530.
11. Scholz IV, Cengic N, Baker CH, et al. Radioiodine therapy of colon cancer following tissue-specific sodium iodide symporter gene transfer. *Gene Ther*. 2005;12:272–280.
12. Dwyer RM, Bergert ER, O'Connor MK, Gendler SJ, Morris JC. In vivo radioiodide imaging and treatment of breast cancer xenografts after MUC1-driven expression of the sodium iodide symporter. *Clin Cancer Res*. 2005;11:1483–1489.
13. Schipper ML, Weber A, Behe M, et al. Radioiodide treatment after sodium iodide symporter gene transfer is a highly effective therapy in neuroendocrine tumor cells. *Cancer Res*. 2003;63:1333–1338.

14. Kang JH, Chung JK, Lee YJ, et al. Establishment of a human hepatocellular carcinoma cell line highly expressing sodium iodide symporter for radionuclide gene therapy. *J Nucl Med*. 2004;45:1571–1576.
15. Faivre J, Clerc J, Gerolami R, et al. Long-term radioiodine retention and regression of liver cancer after sodium iodide symporter gene transfer in Wistar rats. *Cancer Res*. 2004;64:8045–8051.
16. Hart IR. Tissue specific promoters in targeting systemically delivered gene therapy. *Semin Oncol*. 1996;23:154–158.
17. He P, Tang ZY, Ye SL, Liu BB, Liu YK. The targeted expression of interleukin-2 in human hepatocellular carcinoma cells. *J Exp Clin Cancer Res*. 2000;19:183–187.
18. Cao G, Kuriyama S, Du P, et al. Complete regression of established murine hepatocellular carcinoma by in vivo tumor necrosis factor alpha gene transfer. *Gastroenterology*. 1997;112:501–510.
19. Miyatake SI, Tani S, Feigenbaum F, et al. Hepatoma-specific antitumor activity of an albumin enhancer/promoter regulated herpes simplex virus in vivo. *Gene Ther*. 1999;6:564–572.
20. Pinkert CA, Ornitz DM, Brinster RL, Palmiter RD. An albumin enhancer located 10 kb upstream functions along with its promoter to direct efficient, liver-specific expression in transgenic mice. *Genes Dev*. 1987;1:268–276.
21. Nakajima K, Ikenaka K, Nakahira K, Morita N, Mikoshiba K. An improved retroviral vector for assaying promoter activity: analysis of promoter interference in pIP211 vector. *FEBS Lett*. 1993;315:129–133.
22. Haberkorn U, Henze M, Altmann A, et al. Transfer of the human NaI symporter gene enhances iodide uptake in hepatoma cells. *J Nucl Med*. 2001;42:317–325.
23. Haberkorn U, Kinscherf R, Kissel M, et al. Enhanced iodide transport after transfer of the human sodium iodide symporter gene is associated with lack of retention and low absorbed dose. *Gene Ther*. 2003;10:774–780.
24. Haberkorn U, Beuter P, Kübler W, et al. Iodide kinetics and dosimetry in vivo after transfer of the human sodium iodide symporter gene in rat thyroid carcinoma cells. *J Nucl Med*. 2004;45:827–833.
25. Mandell RB, Mandell LZ, Link CJ Jr. Radioisotope concentrator gene therapy using the sodium/iodide symporter gene. *Cancer Res*. 1999;59:661–668.
26. Su H, Lu R, Chang JC, Kan YW. Tissue-specific expression of herpes simplex virus thymidine kinase gene delivered by adeno-associated virus inhibits the growth of human hepatocellular carcinoma in athymic mice. *Proc Natl Acad Sci U S A*. 1997;94:13891–13896.
27. Sieger S, Jiang S, Schönsiegel F, et al. Tumour-specific activation of the sodium/iodide symporter gene under control of the glucose transporter gene 1 promoter (GT1-1.3). *Eur J Nucl Med Mol Imaging*. 2003;30:748–756.
28. Van Sande J, Massart C, Beauwens R, et al. Anion selectivity by the sodium iodide symporter. *Endocrinology*. 2003;144:247–252.
29. Dadachova E, Bouzahzah B, Zuckier LS, Pestell RG. Rhenium-188 as an alternative to iodine-131 for treatment of breast tumors expressing the sodium/iodide symporter (NIS). *Nucl Med Biol*. 2002;29:13–18.
30. Larsen RH, Slade S, Zalutsky MR. Blocking [<sup>211</sup>At]astatide accumulation in normal tissues: preliminary evaluation of seven potential compounds. *Nucl Med Biol*. 1998;25:351–357.
31. Petrich T, Helmeke HJ, Meyer GJ, Knapp WH, Potter E. Establishment of radioactive astatine and iodine uptake in cancer cell lines expressing the human sodium iodide symporter. *Eur J Nucl Med Mol Imaging*. 2002;29:842–854.
32. Carlin S, Akabani G, Zalutsky MR. In vitro cytotoxicity of <sup>211</sup>At-astatide and <sup>131</sup>I-iodide to glioma tumor cells expressing the sodium/iodide symporter. *J Nucl Med*. 2003;44:1827–1838.
33. Shen DH, Marsee DK, Schaap J, et al. Effects of dose, intervention time, and radionuclide on sodium iodide symporter (NIS)-targeted radionuclide therapy. *Gene Ther*. 2004;11:161–169.
34. Zinn KR, Buchsbaum DJ, Chaudhuri TR, Mountz JM, Grizzle WE, Rogers BE. Noninvasive monitoring of gene transfer using a reporter receptor imaged with a high-affinity peptide radiolabeled with <sup>99m</sup>Tc or <sup>188</sup>Re. *J Nucl Med*. 2000;41:887–895.
35. Raben D, Buchsbaum DJ, Khazaeli MB, et al. Enhancement of radiolabeled antibody binding and tumor localization through adenoviral transduction of the human carcinoembryonic antigen gene. *Gene Ther*. 1996;3:567–580.
36. Altmann A, Kissel M, Zitzmann S, et al. Increased MIBG uptake after transfer of the human norepinephrine transporter gene in rat hepatoma. *J Nucl Med*. 2003;44:973–980.
37. Boyd M, Mairs RJ, Keith WN, et al. An efficient targeted radiotherapy/gene therapy strategy utilising human telomerase promoters and radioastatine and harnessing radiation-mediated bystander effects. *J Gene Med*. 2004;6:937–947.
38. Spitzweg C, Dietz AB, O'Connor MK, et al. In vivo sodium iodide symporter gene therapy of prostate cancer. *Gene Ther*. 2001;8:1524–1531.



The Journal of  
NUCLEAR MEDICINE

## Radioiodine Therapy of Hepatoma Using Targeted Transfer of the Human Sodium/Iodide Symporter Gene

Libo Chen, Annette Altmann, Walter Mier, Helmut Eskerski, Karin Leotta, Lihe Guo, Ruisen Zhu and Uwe Haberkorn

*J Nucl Med.* 2006;47:854-862.

---

This article and updated information are available at:  
<http://jnm.snmjournals.org/content/47/5/854>

---

Information about reproducing figures, tables, or other portions of this article can be found online at:  
<http://jnm.snmjournals.org/site/misc/permission.xhtml>

Information about subscriptions to JNM can be found at:  
<http://jnm.snmjournals.org/site/subscriptions/online.xhtml>

*The Journal of Nuclear Medicine* is published monthly.  
SNMMI | Society of Nuclear Medicine and Molecular Imaging  
1850 Samuel Morse Drive, Reston, VA 20190.  
(Print ISSN: 0161-5505, Online ISSN: 2159-662X)

© Copyright 2006 SNMMI; all rights reserved.